Journal of Neuroimmunology 334 (2019) 576996

Contents lists available at ScienceDirect

Journal of Neuroimmunology

journal homepage: www.elsevier.com/locate/jneuroim

Exosomes from adipose-derived stem cells alleviate neural injury caused by microglia activation via suppressing NF-kB and MAPK pathway

Nianhua Feng*, Yanjun Jia, Xiaoxi Huang

Medical research center, Beijing chaoyang hospital, Capital medical university, Beijing, China

ARTICLE INFO

Keywords:
Exosomes
Adipose-derived stem cells
Microglia
Inflammation
Neural injury

ABSTRACT

Activation of microglia cells play critical role in neuroinflammation after brain injury. Exosomes from adipose-derived stem cells (ADSC) possess immunoregulation effect similar with ADSC. We hypothesized that ADSC derived exosomes (ADSC-exosomes) could inhibit the activation of microglia cells and prevent neuroinflammation. We found that ADSC-exosomes could inhibit the activation of microglia cells by suppressing NF-kB and MAPK pathway. Production of inflammatory factors in lipopolysaccharide-stimulated microglia cells decreased significantly when pretreated with ADSC-exosomes. Furthermore, ADSC-exosomes could decrease the cytotoxicity of activated microglia. These results revealed that ADSC-exosomes might be a promising strategy for the therapy of neural injury.

1. Introduction

Large amount of neuronal cell death is a main event after brain injury such as intracerebral hemorrhage (Liu et al., 2019), cerebral ischemia (El et al., 2019), and trauma (Aubrecht et al., 2018), which is harmful for the disease progression and prognosis. Suppressing neuronal cell death greatly reduced brain injury (Aubrecht et al., 2018).

It was reported that neuroinflammation was a major factor for secondary insult after brain injury (Kumar et al., 2019). Microglia cells are resident innate immune cells in central nervous system and play important role in neuroinflammation. Cell debris produced by brain injury activated microglia cells and the later secreted large amount of inflammatory factors, which caused secondary injury to surrounding cells (Helmy et al., 2011; D'Avila et al., 2012; Hassani et al., 2012). Previous study has proved that suppressing excessive microglia activation could protect neuronal cells from injury (Ni et al., 2019).

Adipose-derived stem cell (ADSC) is a kind of adult stem cell isolated from adipose tissue. Many studies have shown that ADSC transplantation was an effective therapy for tissue repair and regeneration (Zhao et al., 2017; Bruun et al., 2018; Gadelkarim et al., 2018; Lauritano et al., 2018; Hassanshahi et al., 2019). However, different from the initial concept that ADSC promoted tissue recovery by replacing lost tissues, more and more recent evidences suggested that ADSC participated in tissue repair by secreting factors such as vascular endothelial growth factor (VEGF), hepatocyte growth factor (HGF), insulin-like growth factor (IGF), basic fibroblast growth factor (bFGF) (Liang et al., 2014). Exosomes are extracellular microvesicles that secreted by almost all type of cells, they carried large number of bioactive molecules including RNA, protein, lipids, which produced by original cells and mediated communications between cells (Wu et al., 2018). It was reported that ADSC derived exosomes (ADSC-exosomes) had similar effect on immunoregulation as ADSC (Doeppner et al., 2015), which meant that exosomes may possess the biological functions of original cells. Thus, we proposed that ADSC-exosomes could inhibit the inflammatory responce mediated by microglia activation and reduced neuronal cell death caused by inflammatory factors derived from activated microglia cells.

In this study, ADSCs were isolated from adult SD rat donor and amplified for several passages before use. ADSC-exosomes were purified from cell culture supernatant through ultracentrifugation. Lipopolysaccharide (LPS) stimulated BV2 cells (a microglia cell line) were used as cell model to mimic neuroinflammation. To identify the function of ADSC-exosomes on BV2 activation, ADSC-exosomes were cocultured with LPS-stimulated BV2 cells, RNA, protein and cell supernatant were collected 6 h later. The production of inflammatory factors were detected. Then, the supernatant of BV2 cells after different

Abbreviation: ADSC, adipose-derived stem cell; LPS, lipopolysaccharide; NF-kB, nuclear factor kappa B; MAPK, mitogen activated protein kinase; CCK8, cell counting kit; NTA, nano tracking analysis

* Corresponding author at: Medical research center, Beijing chaoyang hospital, Capital medical university, 8# Gongti south street, Chaoyang district, Beijing 100020, China.

E-mail address: leanne02@163.com (N. Feng).

https://doi.org/10.1016/j.jneuroim.2019.576996
Received 5 March 2019; Received in revised form 23 April 2019

treatment were collected and cocultured with human neuroblastoma cell line SH-SY5Y, cell viability was measured to detect the neural injury. Finally, the activation of NF-kB and MAPK pathway, two important signal pathways in inflammation was examined and mechanisms were investigated.

2. Materials and methods

2.1. Cell culture

The murine microglia cell line BV-2 and human neuroblastoma cell line SH-SY5Y were purchased from the Cell Resource Center, Peking Union Medical College (which is the headquarters of National Infrastructure of Cell Line Resource, NSTI). Both cell lines were cultured in dulbecco's modified eagle's medium (DMEM) (Gibco, Grand island, NY, USA) supplemented with 10% fetal bovine serum (FBS) (Hyclone, South America) at 37 °C with 5% CO2 saturation. Passages were performed every three days at a ratio of 1:3–6 for BV2 and 1:3 for SH-SY5Y. To induce the activation of BV2 cells, 25 ng/ml LPS was added to the culture medium and incubated for 6 h. To explore the effect of ADSC-exosomes on BV2 activation, BV2 cells were cocultured with ADSC-exosomes for 2 h before incubated with 25 ng/ml LPS (Sigma-Aldrich, Shanghai, China) for 6 h. Total RNA, protein and cell supernatant were collected for the following detection.

2.2. Isolation and culture of adipose-derived stem cell (ADSC)

All experiments were approved by the animal ethic committee of capital university of medical sciences. SD rats (8-12 W) were provided by beijing vital river laboratory animal technology Co., Ltd. Fat tissues in the inguinal region were used for the isolation of ADSC according to a previously described method with small modification (Zhang et al., 2014). Briefly, aseptically harvested fat tissues were washed in phosphate buffered solution (PBS) for three times and finely minced. Then, the fat tissues were digested with 1% collagenase type Iat 37 °C in a shaker. 40 min later, the digested tissues were filtered through a 70 μm filter and centrifuged at 1500 rpm for 10 min, after being washed for another two times, the pellet was resuspended in complete medium (DMEM containing 10% FBS and 100 U/ml penicillin/streptomycin) and plated in 10 cm cell culture dishes, the medium was replaced every 2–3 days. Passages were performed when cells were 80–90% confluence.

2.3. Characterization of surface markers of ADSC by flow cytometry

Specific surface markers expressed in rat ADSC were detected by flow cytometry. Briefly, ADSCs were detached and collected by centrifuging at 1200 rpm for 5 min. Total cell number was counted and then transfered to new tubes (10^6 cells/tube), all cells were incubated with the following antibodies against CD45-eFluor450, CD31-eFluor660, CD90-FITC, CD29-FITC. Isotype control staining was performed using mouse-IgG1 kappa eFluor450, mouse-IgG1 kappa eFluor660, mouse-IgG2a kappa FITC and armenian Hamster-IgG FITC (all from Thermo Fisher scientific, San Diego, CA) in the dark at 4 °C for 30 min. Then, cells were washed twice in PBS. Samples were detected using BD canto II flow cytometer and analyzed by FlowJo software.

2.4. Multi-potential differentiation of rat ADSC

For adipogenesis, ADSCs were seeded in 24 well-plate at a density of 2×10^4 cells/cm^2, when cells were 100% confluence, medium was changed into adipogenesis medium A (Cyagen, Guangzhou, China) (Medium A contains 175 ml basic medium A, 20 ml FBS, 2 ml glutamine, 2 ml penicillin-streptomycin, 400 μl linsulin, 200 μl 3-isobuty-1-methylxanthine, 200 μl rosiglitazone and 200 μl dexamethasone). 3 days later, medium A was changed into medium B (Cyagen, Guangzhou, China) (Medium B contains 175 ml basic medium B, 20 ml FBS, 2 ml penicillin-streptomycin, 2 ml glutamine and 400 μl insulin) and cultured for 24 h, then, medium was changed back to medium A. After 3–5 cycles, cells were cultured in medium B for additional 4–7 days, and intracellular lipid accumulation was observed by staining with Oil red O (Sigma-Aldrich, Shanghai, China).

For osteogenic differentiation, ADSCs were plated in 0.1% gelatin-coated 24 well-plate at a density of 2×10^4 cells/cm^2. When cells were 60–70% confluence, culture medium was changed into osteogenic differentiation medium (Cyagen, Guangzhou, China) (Osteogenic differentiation medium contains 175 ml basic medium, 20 ml FBS, 2 ml penicillin-streptomycin, 2 ml glutamine, 400 μl ascorbate, 2 ml β-Glycerophosphate and 20 μl dexamethasone) and replaced every 2–3 days, after 14–28 days, osteogenesis potential was characterized by alizarin red (Cyagen, Guangzhou, China) staining.

For chondrogenic differentiation, ADSCs were detached and collected by centrifuging at 1200 rpm for 5 min, 5×10^5 cells were resuspended in chondrogenic differentiation medium (Cyagen, guangzhou, China) (Chondrogenic differentiation medium contains 194 ml basic medium, 600 μl ascorbic acid, 20 μl dexamethasone, 2 ml insulin-tranferrin-selenium (ITS) supplement, 2 ml TGF-β3, 200 μl proline and 200 μl sodium pyruvate) and transfer into a polypropylene tube, cells were centrifuged at 1200 rpm for 5 min again to form cell pellet, which was benefit for chondrogenesis. Cell pellets were cultured in tubes with loose caps at 37 °C, medium was changed every 2–3 days. Chondrogenic pellets were harvested after 14–28 days' culture and detected by alcian blue (Cyagen, Guangzhou, China) staining.

2.5. Isolation and identification of rat ADSC-exosomes

2.5.1. Isolation of rat ADSC-exosomes

Exosomes were extracted from the supernatant of rat ADSCs by ultracentrifugation. First, when reached 70–80% confluence, ADSCs at passage 3–5 were cultured in DMEM supplement with 10% exosome-free FBS (exosome-free FBS was obtained by ultracentrifuged at 100000 g for 16 h) for another 48 h before harvesting the medium. Second, the supernatant was centrifuged at 500 g for 10 min followed by 12,000 g for 20 min at 4 °C to remove cell debris and apoptosis bodies. Then the medium was filtered through a 0.22 μm filter. Finally, exosomes in the culture medium were isolated by ultracentrifuging at 100000 *g* for 70 min. Pellet was resuspended in PBS and kept in −80 °C for long term storage.

2.5.2. The internalization of ADSC-exosomes by BV2 cells

To detect the internalization of ADSC-exosomes by BV2 cells, ADSC-exosomes were resuspended with PBS containing 5 μM DiI (Sigma-Aldrich, Shanghai, China) and incubated for 15 min at 37 °C, excess dye was neutralized with 1 ml 5% BSA and washed by ultracentrifugation. DiI-labeled ADSC-exosomes were cocultured with BV2 cells for 24 h. Cells were fixed with 4% paraformaldehyde and counterstained with DAPI (Sigma-Aldrich, Shanghai, China), then samples were observed and images were taken under a confocal microscope (Leika,Germany).

2.5.3. Transmission electron microscopy detection of rat ADSC-exosomes

ADSC-exosomes were fixed with 2% paraformaldehyde and 2% glutaraldehyde, then samples were absorbed onto a carbon-coated copper grid and negative stained with 2% uranyl acetate for examination using a TEM (JEM-1400 plus; JEOL Ltd., Japan) at 80 kV.

2.5.4. Nanopartical tracking analysis (NTA)

To analyze the size distribution of ADSC-exosomes, ADSC-exosomes were resuspended in PBS and analyzed using zetaview (particle metrix, Germany). Diameter of particles were analyzed using ZetaView 8.04.02 software.

Table 1
Primer information.

Gene	Forward	Reverse
IL-1β	GAAATGCCACCTTTTGACAGTG	TGGATGCTCTCATCAGGACAG
IL-6	CTGCAAGAGACTTCCATCCAG	AGTGGTATAGACAGGTCTGTTGG
TNF-α	ACCCTCACACTCACAAACCAC	ACAAGGTACAACCCATCGGC
iNOS	TCCCTTCCGAAGTTTCTGGC	CTCTCTTGCGGACCATCTCC
COX-2	TGGGGGAAGAAATGTGCCAA	AGAAGCGTTTGCGGTACTCA
GAPDH	GGAGAGTGTTTCCTCGTCCC	ACTGTGCCGTTGAATTTGCC

2.6. RNA isolation and quantitative real-time polymerase chain reaction (qRT-PCR)

Total RNA was extracted using TRIzol reagent (Thermo Fisher Scientific, Carlsbad, CA, USA) and treated with DNase I (Transgen Biotech, Beijing, China). First-strand cDNA was synthesized with 1 μg total RNA in 20 μl using a TransScript First-Strand cDNA Synthesis SuperMix (Transgen Biotech, Beijing, China) according to the manufacturer's instruction. Quantitative real-time polymerase chain reaction (qPCR) analysis was performed in triplicate using SYBR Premix Ex Taq II (Takara, Dalian, China), and gene expression was detected using LightCycler 480 II (Roche, mannheim, Germany). The thermal parameters were 95 °C for 30s, followed by 40 cycles of 95 °C for 5 s and 60 °C for 30 s, then, 95 °C for 5 s and 50 °C for 30 s. Gene expression level was normalized by GAPDH housekeeping gene expression. The primer sequences used in our study were listed in Table 1.

2.7. Enzyme-linked immunosorbent assay (ELISA)

To detect the concentration of inflammatory factors secreted by BV2 cells, culture medium was collected, the secretion of tumor necrosis factor alpha (TNF-α) and interleukin 6 (IL-6) were assayed by enzyme-linked immunosorbent assay kits according to the manufacturer's instructions (R&D system, minneapolis, USA).

2.8. Cell viability detection

To compare the effect of BV2 condition medium in different group on SH-SY5Y, SH-SY5Y were cultured in cell supernatant of BV2 cells and cell viability was determined by cell counting kit 8 (CCK8) assay (KeyGEN BioTECH, Nanjing, China). Briefly, SH-SY5Y cells were seeded in 96 well plate at 20000 cell per well and cultured in cell culture supernatant of BV2 cells from different groups for 24 h. Then CCK8 was added and incubated for 2 h. Optical density (OD) was measured at 450 nm using a microplate reader (Thermo scientific, USA). Cell viability was showed as OD and presented as mean ± SD. Cell number in BV2 group without any treatment was regarded as control group, viable cell rate was caculated according to the following formula: viable cell rate = (OD(experiment group)-OD(background))/(OD(control group)-OD(background)) × 100%.

2.9. Western blot analysis

Western blot was performed to detect the expression of exosomal markers and the activation state of NF-kB and MAPK signal pathway. Briefly, ADSC-exosomes or BV2 cells treated with LPS or LPS + ADSC-exosomes for 0, 15 min, 30 min and 1 h were collected and lysed with RIPA buffer (Beyotime, Beijing, China), after centrifuged at 12000 rpm for 30 min at 4 °C, the supernatant were collected for quantification using BCA detection kit (Beyotime, Beijing, China). Then, samples were separated with 10% SDS-PAGE (Beyotime, Beijing, China) and proteins were transferred to PVDF membrane (Millipore, Germany). The membrane was blocked with 5% non-fat milk for 1 h and incubated with primary antibodies overnight at 4 °C, followed by incubation of corresponding horseradish peroxidase-conjugated secondary antibodies for 1 h at room temperature. The protein expression was colored with ECL substrate (Millipore, Germany) and detected with a BG-gdsAUTO710 Mini chemiluminescence imaging system (BAYGENE, Beijing, China). The following primary antibodies were used: rabbit anti-P44/42 MAPK (ERK1/2), anti-phospho-P44/42 MAPK (p-ERK1/2), anti-JNK, anti-phospho-SAPK/JNK (p-JNK), anti-NF-kB P65 (P65), anti-phospho-NF-kB P65 (p-P65), anti-P38 MAPK (P38), anti-phospho-P38 MAPK (p-P38), mouse anti-β-actin (Cell Signaling Technology, Shanghai, China), anti-CD63 (Santa cruz, Shanghai, China), anti-CD9 (Abcam, Cambridge, MA, USA), anti-TSG101 (Abcam, Cambridge, MA, USA). Secondary antibodies were horseradish peroxidase-conjugated goat anti-rabbit IgG (H + L), horseradish peroxidase-conjugated goat anti-mouse IgG (H + L) (Zhongshanjinqiao, Beijing, China).

2.10. Statistical analysis

All experiments were performed three times. Data were presented as mean ± SD. Statistical significance was tested by two-tailed Student's t-test using SPSS statistics 17.0. A value of $P < 0.05$ was considered statistically significant (indicated by "*").

3. Results

3.1. Characterization of rat ADSCs

After 24 h in culture, primary ADSCs adhered to the culture dishes. These cells proliferated rapidly and grew as clonies, most of cells displayed typical spindle-shaped cell body. After the first dissociation, passage was performed every other day. After 2–3 passages, all cells exhibited a uniform fibroblast-like morphology (Fig. 1A). All ADSCs were positive for CD90 and CD29, but negative for CD31 and CD45 (Fig. 1B). When cultured in differentiation condition for adipogenesis, osteogenesis and chondrogenesis for 2–4 weeks, ADSCs could differentiate into adipocytes, osteocytes and chondrocytes, which confirmed by oil red, alizarin red and alcian blue staining respectively (Fig. 1C). Thus, cells isolated from adipose tissues in our study possessed the characteristics of ADSCs.

3.2. Identification of ADSC-exosomes

ADSC-exosomes presented as round particals with typical cup-shape morphology when observed by electron microscopy (Fig. 2A). Nano tracking analysis (NTA) showed that ADSC-exosomes had a vesicle diameter ranging from 30 to 150 nm(Fig. 2B). Exosomal markers were also detected by western blot analysis, which showed that exosomes expressed CD9, CD63 and TSG101 (Fig. 2C). After incubated in medium contained DiI-labeled exosomes for 24 h, strong red fluorescence was detected around the nucleus of BV2 cells (Fig. 2D), which meant that exosomes could enter into BV2 cells and be internalized.

3.3. ADSC-exosomes suppressed the activation of LPS-stimulated BV2 cells

Microglia are major immune cells in nervous system and played important role in neuroinflammation, once being activated, microglia cells could secret several kinds of inflammatory factors such as IL-1β, IL-6, TNF-α and so on (Jaimes et al., 2017). Here, we detected the function of ADSC-exosomes on microglia activation. BV2 cells exposed to LPS were used as cell model of micorglia activation. All cells cultured in DMEM containing 10% FBS were divided into 4 groups: control group (BV2 cells without treatment), exosomes group (BV2 cells incubated with 50 μg/ml ADSC-exosomes), LPS group (BV2 cells treated with 25 ng/ml LPS), LPS + exosomes group (BV2 cells were pretreated with 50 μg/ml ADSC-exosomes for 2 h and then treated with 25 ng/ml LPS for another 6 h). Total RNA and cell supernatant were collected for the following detection. Expression of genes encoding inflammatory factors IL-1β, IL-6, TNF-α, iNOS and Cox2 were evaluated by

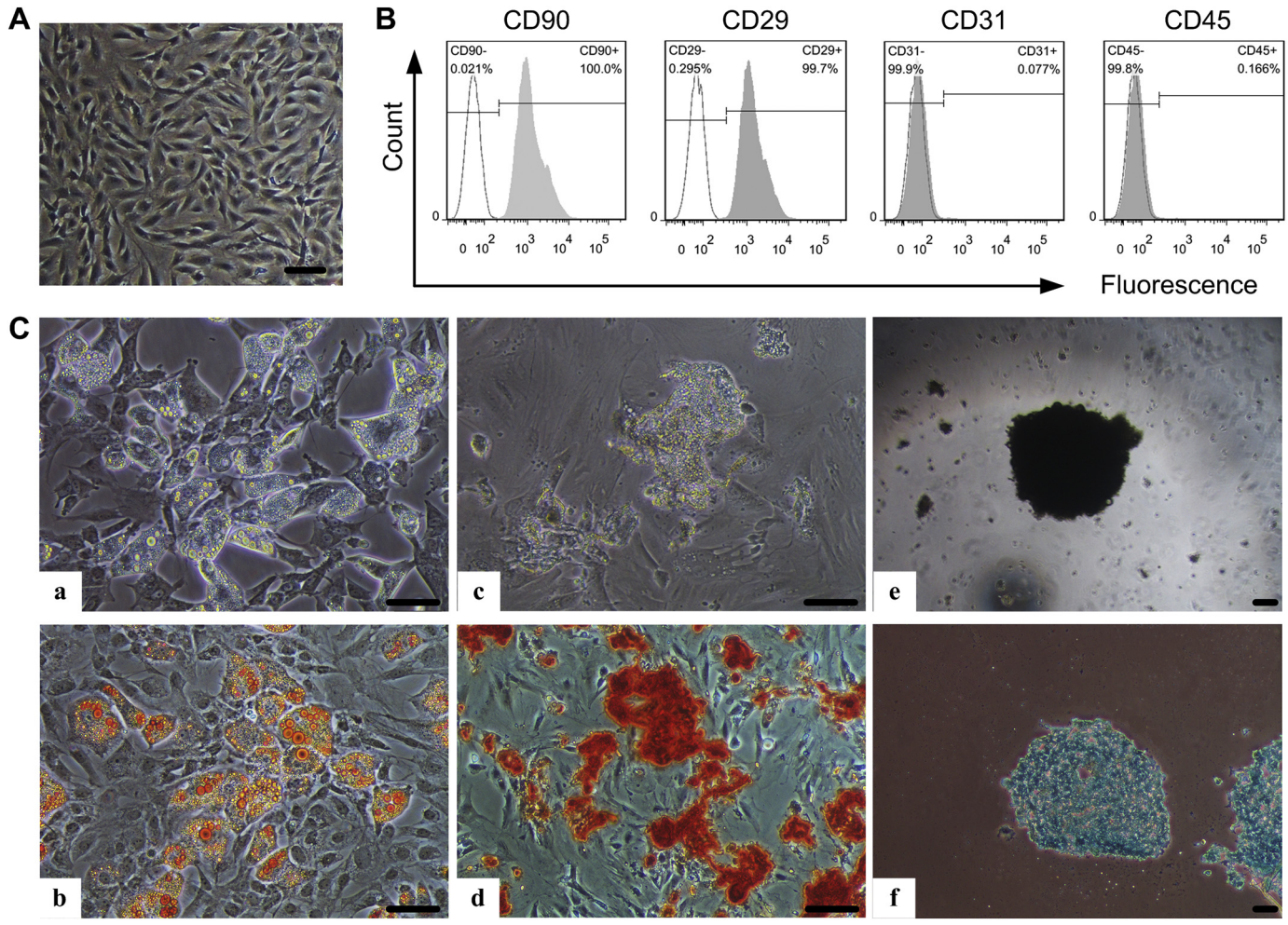

Fig. 1. Identification of rat adipose-derived stem cell (ADSC) (bar = 50 μm). (A) ADSC at the third passage exhibited a fibroblast-like morphology. (B) Detection of the specific markers of ADSCs by flow cytometry showed that ADSCs were positive for CD90 and CD29, negative for CD31 and CD45. (C) Multi-differentiation potential of ADSCs. (a-b) 2 weeks after cultured in adipogenesis medium, ADSCs differentiated into adipocytes which contained large amount of oil-red O positive lipid droplets. (c-d) ADSCs could differentiate into osteoblast cells and formed mineralzation nodes which could be stained by alizarin red. (e-f) when cultured in chondrogenesis medium, ADSCs aggregated and differentiated into alcian blue positive chondrocytes. (For interpretation of the references to colour in this figure legend, the reader is referred to the web version of this article.)

quantitative real-time PCR. ELISA was used to detect the secretion of inflammatory factors TNF-α and IL-6 in cell supernatant. We found that gene expression of IL-1β, IL-6, TNF-α, iNOS and Cox2 in BV2 cells increased significantly after exposed to LPS. However, the gene expression of inflammatory factors in BV2 cells were much lower in LPS + exosomes group than LPS group. No difference was observed between BV2 cells (control group) and BV2 cells treated with ADSC-exosomes only (exosomes group) (Fig. 3A). Similar with gene transcription, the secretion of IL-6 and TNF-α in cell supernatant also increased after LPS exposure. However, compared with LPS group, lower concentration of IL-6 and TNF-α was detected in LPS + exosomes group, that was 310.81 ± 5.24 pg/ml and 100.81 ± 2.86 pg/ml for IL-6, 1859.39 ± 10.87 pg/ml and 1212.91 ± 65.42 pg/ml for TNF-α respectively (Fig. 3B).

3.4. ADSC-exosomes decreased the toxicity of LPS-exposed BV2 cells

It was reported that over-activated microglia cells could secret large amount of inflammatory factors which were toxic to surrounding cells (Block et al., 2005). Suppressing the activation of microglia cells could protect cells from injury (Hsuan et al., 2016). To further determine the influence of ADSC-exosomes on the toxicity of activated BV2 cells, we detected the cytotoxic effect of cell supernatant of BV2 cells on the survival of SH-SY5Y cells. SH-SY5Y cells were cultured in cell supernatant of BV2 cells from four groups mentioned above. 24 h later, we observed that cells were prone to reteacted and turned round in exosomes group, LPS group and LPS + exosomes group. Compared to control group and exosomes group, there was a significant decrease of cell number in LPS and LPS + exosomes group, lot of dead cells and cell debris were found in LPS group, and most of viable cells turned round. Compared to LPS group, there were fewer dead cells and more viable cells in LPS + exosomes group (Fig. 4A). CCK8 was added into culture medium and optical density (OD) was measured in each group. We found that, similar with the observation under microscope, decreased cell viability were observed in both LPS and LPS + exosomes group. Compared to LPS group, cell viability in LPS + exosomes group was much higher, that meant less cytotoxicity. No difference was detected between control and exosomes group (Fig. 4B). Cell supernatant of activated BV2 cells was less cytotoxic in the presence of exosomes, may be because of that exosomes suppressed the activation of BV2 cells and inhibited the expression and protein secretion of inflammatory factors which were toxic to neural cells.

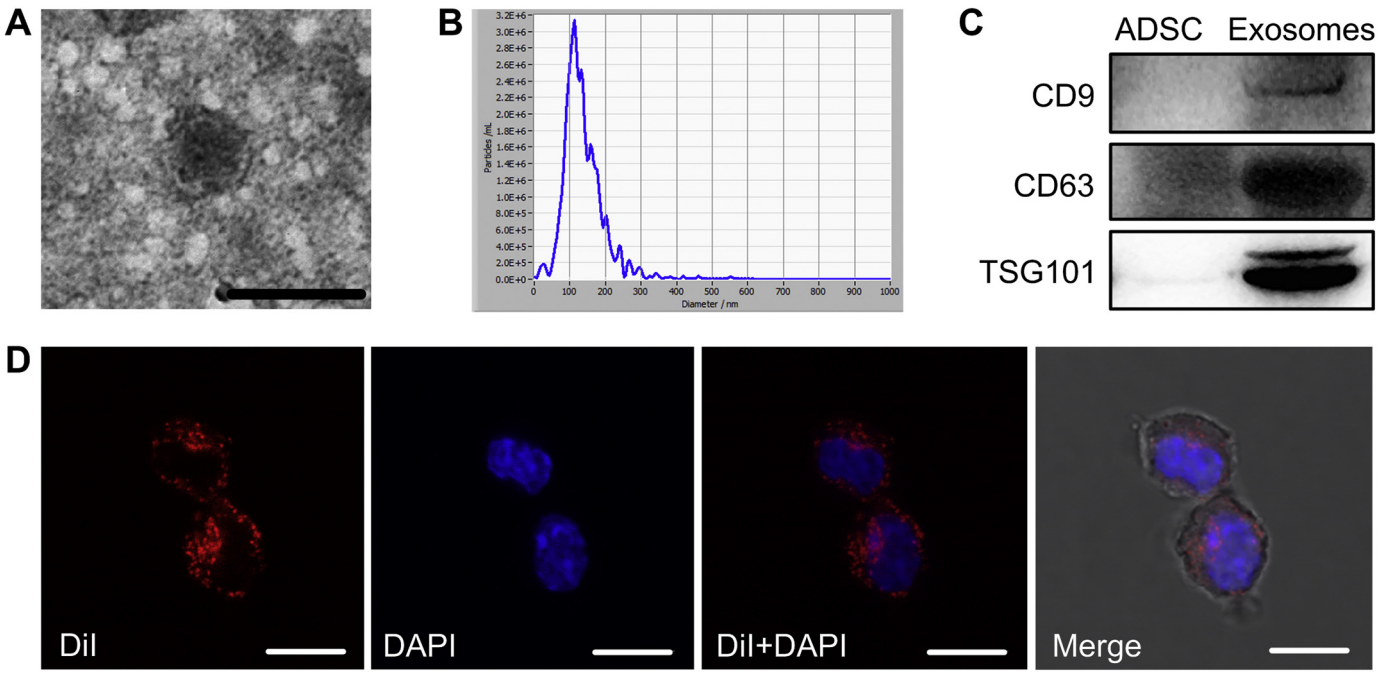

Fig. 2. Identification of ADSC-exosomes. (A) ADSC-exosome was round vesicle with typical cup-shape morphology by transmission electron microscopy analysis (bar = 100 nm). (B) Size distribution was measured by zetaview, ADSC-exosomes had a vesicle diameter ranging from 30 to 150 nm. (C) Western blot analysis showed that ADSC-exosomes expressed CD9, CD63, TSG101. (D) By confocal microscope imaging, we observed that Dil-labeled exosomes (red) could enter into BV2 cells and mainly localized around the nucleus(blue) (DAPI stained) (bar = 10 μm). (For interpretation of the references to colour in this figure legend, the reader is referred to the web version of this article.)

3.5. ADSC-exosomes inhibited neuroinflammation by suppressing NF-kB and MAPK signal pathway

To investigate the potential mechanism by which ADSC-exosomes inhibited neural injury, we detected the activation of NF-kB and MAPK signal pathway, two important pathways for inflammatory reaction, by western blot analysis. It was reported that NF-kB and MAPK signal pathway modulated the gene expression of proinflammatory cytokines such as IL-1β, TNF-α and IL-6 (Jaimes et al., 2017; Li et al., 2018a; Wang and Han, 2018). To determine the influence of ADSC-exosomes on the activation of NF-kB and MAPK signal pathway, BV2 cells were divided into 7 groups: control group (BV2 cells without any treatment), LPS 15 min group (BV2 cells treated with 25 ng/ml LPS for 15 min), LPS + E 15 min group (BV2 cells pretreated with ADSC-exosomes for 2 h and then treated with 25 ng/ml LPS for 15 min), LPS 30 min group (BV2 cells treated with 25 ng/ml LPS for 30 min), LPS + E 30 min group (BV2 cells pretreated with ADSC-exosomes for 2 h and then treated with 25 ng/ml LPS for 30 min), LPS 1 h group (BV2 cells treated with 25 ng/ml LPS for 1 h), LPS + E 1 h group (BV2 cells pretreated with ADSC-exosomes for 2 h and then treated with 25 ng/ml LPS for 1 h), proteins were collected in each group and the expression of NF-kB P65, phosphorylated P65 (p-P65), ERK, phosphorylated ERK (p-ERK), JNK, phosphorylated JNK (p-JNK), P38, phosphorylated P38 (p-P38) were detected by western blot analysis. We observed that, after LPS exposure, the phosphorylation of NF-kB P65 (p-P65, an important molecule in NF-kB pathway) and ERK, JNK, P38 (three subgroups of MAPK signal pathway) increased significantly and reached to the peak at different time, which meant that NF-kB and MAPK signal pathway were all activated and taken part in the activation of BV2 after LPS treatment. The phosphorylation of P65 and ERK increased immediately after exposed to LPS for 15 min, phosphorylation of JNK also increased after 15 min stimulation by LPS and reached to peak at 30 min. Differently, phosphorylation of P38 begin to increase after 30 min LPS-exposure and then declined gradually as time extended. Furthermore, we found that the phosphorylation of P65, ERK, JNK and P38 was lower in LPS + E group after exposed to LPS for 15 min or 30 min (Fig. 5). Obviously, ADSC-exosomes could suppress the activation of NF-kB and MAPK signal pathway, and consequently influenced the transcription of genes downstream such as IL-1β, IL-6, TNF-α, iNOS and Cox2.

4. Discussion

Microglia cells are important immune cells in central nervous system. However, excessive or constant activation of microglia was one of the main factor leading to neural injury (Kumar et al., 2019; Lee et al., 2019), which is bad for recovery of injury. In this study, we found that ADSC-exosomes could suppress the activation of BV2 cells by decreasing the activation of NF-kB and MAPK signal pathway, thus attenuated gene expression and protein secretion of inflammatory factors such as TNF-α, IL-6, IL-1β, iNOs and Cox2, and protected neural cells from injury caused by inflammatory factors derived from activated BV2 cells.

Neuroinflammation is a reply against various stimulus and harmful molecules in the process of neural injury, and It has been considered as a critical mechanism responsible for acute and chronic neural diseases or neural injury, such as traumatic brain injury (Ni et al., 2019), cerebral ischemia/reperfusion (Xu et al., 2018) and neurodegenerative diseases (Calsolaro et al., 2016). Microglia are resident macrophages in central nervous system and mainly function on monitoring the health state of central nervous system (Waisman et al., 2015). It was considered that microglia were highly related with neuroinflammation of central nervous system. In healthy central nervous system, microglia kept “resting” state and was mainly responsible for maintainance of homeostasis by removing debris and apoptotic cells (Nimmerjahn et al., 2005; Koizumi et al., 2007; Sierra et al., 2010). Once the homeostasis of neural microenviroment was broken by neural injury or neurodegenerative diseases, microglia were exposed to various stimulus and being activated, modest activation of microglia was helpful for tissue repair (Davalos et al., 2005; Nimmerjahn et al., 2005), however, excessive and prolonged activation may cause serious neuroinflammation which

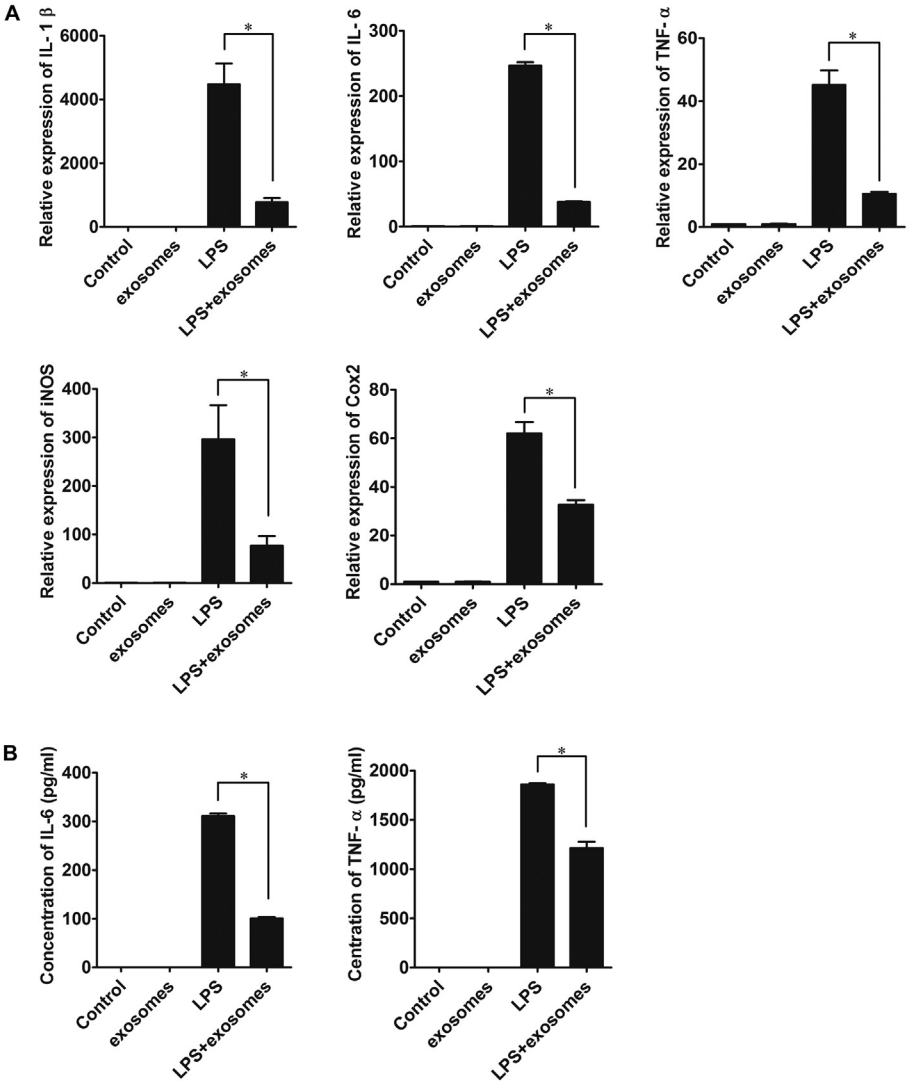

Fig. 3. ADSC-exosomes suppressed LPS-induced activation of BV2 cells. (A) qRT-PCR detection showed that ADSC-exosomes inhibited the increase of gene expression of IL-1β, IL-6, TNF-α, iNOS and Cox2 in LPS-exposed BV2. (B) Compared to LPS group, there were less IL-6 and TNF-α in cell supernatant of BV2 cells in LPS + exosomes group. Control group (BV2 cells without treatment), exosomes group (BV2 cells incubated with ADSC-exosomes), LPS group (BV2 cell treated with 25 ng/ml LPS), LPS + exosomes group (BV2 cells were pretreated with 50 μg/ml ADSC-exosomes for 2 h and then treated with 25 ng/ml LPS for another 6 h) (*P < 0.05).

could be cytotoxic and harmful to neighboring cells, and promoted the apoptosis of neural cells, all these caused secondary brain injury (Atangana et al., 2017; Li et al., 2018c), which was closely related with the prognosis of brain injury. Preventing the activation of microglia greatly decreased the concentration of inflammatory factors in micro-enviroment and improved cell viability (Wu et al., 2017; Atangana et al., 2017; Li et al., 2018a). In this study, we also observed that activated microglia secreted inflammatory factors and promoted the apoptosis of neural cells, while decreased expression of inflammatory factors greatly alleviated neural death, which was similar with previous report (Wu et al., 2017). Thus, inhibition of microglia induced neuroinflammation may be benificial for prevention and therapy for neural injury or degenerative disease caused by neuroinflammation.

Adipose-derived stem cells have been widely used in experimental and preclinical studies and became a promising seed cells of stem cell-based therapy, it was effective in the treatment of various tissue injury or diseases, such as cerebral ischemic injury (Liu et al., 2014), cardiovascular disease (Bruun et al., 2018), graft versus host disease (Fang et al., 2007). It was verified that transplanted ADSC could home to the injury area and replace the host tissues or modulate immune responce (Tajiri et al., 2014). However, in recent years, more and more evidences suggested that the therapeutic effect of ADSC mainly derived from the paracrine factors. The extracellular vesicles were reported to have the main functions in delivering paracrine factors or other bioactive informations between cells (Yang et al., 2018; Li et al., 2018b; Lee et al., 2018; Pan et al., 2019). Exosomes are a kind of endosome-derived extracellular vesicles secreted by almost all type of living cells, 30-150 nm in diameter (Pedersen et al., 2017). They contained information of protein, RNA and lipids from original cells and played important role in cell-cell communication (Lener et al., 2015). After being secreted into extracellular space, exosomes delivered cargos to other cells and altered the function of target cells. There was evidence showed that ADSC-derived exosomes exerted therapeutic effects as ADSC in treating Alzheimer's disease (Ma et al., 2013; Lee et al., 2018). Others also observed that exosomes could pass through the blood brain barrier (BBB), enter into injury area and participate in neurogenesis, angiogenesis and regulate the immune responce to improve the microenviroment of injury area, all of these promoted the recovery of brain injury (Yang et al., 2017; Han et al., 2018; Ni et al., 2019). Here, we found that ADSC-exosomes greatly suppressed the activation NF-kB and MAPK signal pathway in LPS-stimulated BV2 cells and prevented the secretion of inflammatory factors consequently, all of these decreased the toxicity of activated BV2 and protected neural cells from injury. Interestingly, the pretreatment of exosomes have no effect on BV2 cells and didn't activate BV2 cells, as we didn't detect the increased gene transcription and protein secretion of inflammatory factors. This led to the explanation that exosomes only functioned in the process of BV2 activation and have no influence for the “resting state” of microglia cells, that meant fewer side effects.

Though the molecule mechanisms of the effect exert by ADSC-

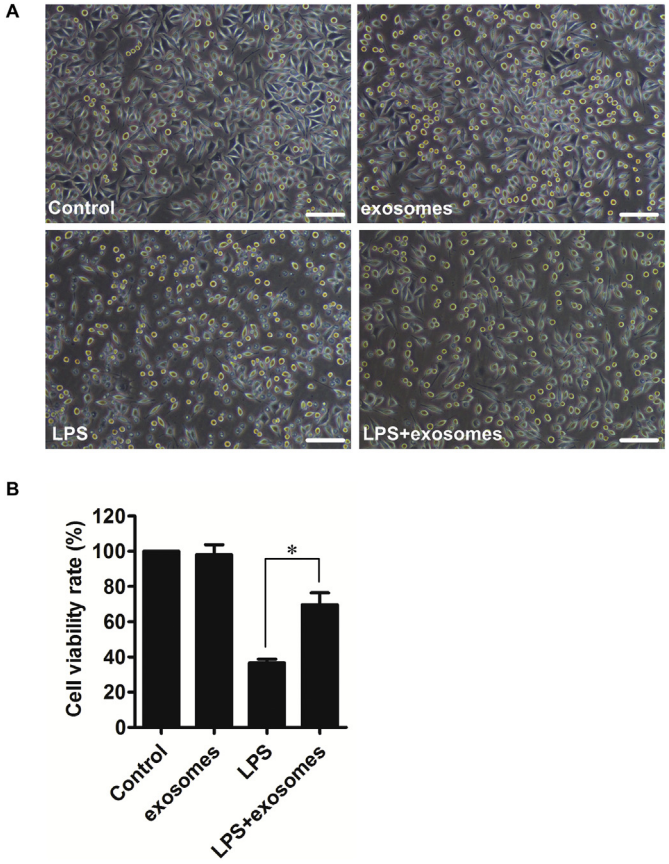

Fig. 4. The influence of ADSC-exosomes on the cytotoxic effect of LPS-exposed BV2 cells. (A) The morphology of SH-SY5Y cultured in the cell supernatant of BV2 cells with different treatment (bar = 100 μm). (B) Cell viability of SH-SY5Y cultured in cell supernatant of BV2 cells with different treatment were examined by CCK8 assay, there were more viable cells in LPS + exosomes group than LPS group. (control: SH-SY5Y cultured in cell supernatant of BV2 cells; exosomes: SH-SY5Y cultured in cell supernatant of BV2 cells which were incubated with ADSC-exosomes; LPS: SH-SY5Y cultured in cell supernatant of BV2 cells which were treated with 25 ng/ml LPS; LPS + exosomes: SH-SY5Y cultured in cell supernatant of BV2 cells which were pretreated with 50 μg/ml ADSC-exosomes for 2 h and then treated with 25 ng/ml LPS for another 6 h)(* $P < 0.05$).

exosomes needs further investigation owing to its complex components, ADSC-exosomes are still considered as the promising substitute for ADSC as a novel cell-free therapeutic strategy in disease therapy, especially for brain injury and neurodegenerative diseases. Compare to ADSC transplantation in the repair of brain injury, ADSC-exosomes have several advantages. First, ADSC-exosomes are convenient to store and use. ADSC-exosomes can be prepared as product, stored in low tempreture and used when needed. Second, it is efficient to use ADSC-exosomes than ADSC in the early stage of injury. It was reported that there were low survival rate of transplanted cells because of the toxic inflammatory and hypoxic microenviroment in the early stage of the injury (Lv et al., 2017a; Zhang et al., 2017; Lv et al., 2017b), which greatly decreased the effect of transplantation. By contrast , exosomes were much stable in the microenviroment of injuried area due to their protective lipid bilayer, and can deliver cargos into target cells directly to promote tissue recovery (Ratajczak et al., 2006; Peinado et al., 2012; Hoshino et al., 2015; Tominaga et al., 2015). Third, ADSC-exosomes can be modified. Molecule such as miRNA, shRNA which were benifit for tissue repair could be loaded into exosomes and delivered into target cells to promote tissue repair (Wang et al., 2018; Yang et al., 2019).

Though have many advantages, it is the begining and still have a long way to go before ADSC-exosomes applied in tissue repair. However, there remained several questions, such as, what is the molecule mechanisms they effect? How to define the effectual dosage of ADSC-exosomes used in disease therapy and how to monitor the quality? How to keep consistency and stability of ADSC-exosomes between batches, between different labs during preparation, and how to supervise? All of these need further investigation.

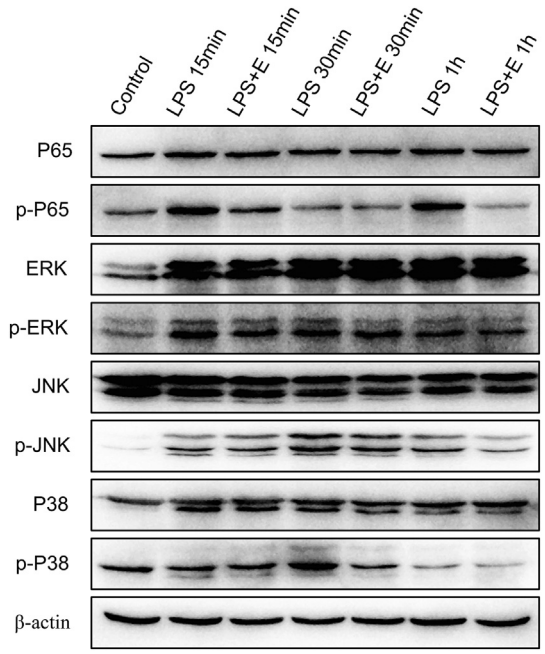

Fig. 5. Western blot analysis showed that ADSC-exosomes suppressed the activation of NF-kB and MAPK signal pathway in BV2 cells. Compared to LPS-treated BV2 cells (LPS group), BV2 cells pretreated with ADSC-exosomes (LPS + E group) exhibited a lower phosphorylation of NF-kB and MAPK after exposed in LPS for 15 min (p-P65 and p-ERK) or 30 min (p-JNK and p-P38). Control group (BV2 cells without any treatment), LPS 15 min group (BV2 cells treated with 25 ng/ml LPS for 15 min), LPS + E 15 min group (BV2 cells pretreated with ADSC-exosomes for 2 h and then treated with 25 ng/ml LPS for 15 min), LPS 30 min group (BV2 cells treated with 25 ng/ml LPS for 30 min), LPS + E 30 min group (BV2 cells pretreated with ADSC-exosomes for 2 h and then treated with 25 ng/ml LPS for 30 min), LPS 1 h group (BV2 cells treated with 25 ng/ml LPS for 1 h), LPS + E 1 h group (BV2 cells pretreated with ADSC-exosomes for 2 h and then treated with 25 ng/ml LPS for 1 h).

Funding sources

This research was supported by the Beijing Municipal Natural Science Foundation (NO.7164261) and Basics-Clinical Research Cooperation Fund of Capital Medical University (NO.16JL31).

Author contributions

Nianhua Feng conceived the study, designed and performed the experiment, wrote the manuscript; Yanjun Jia supervised the study and provided technical support for several experiments; Xiaoxi Huang supervised the study and provided some of reagents;.

Declaration of Competing Interest

The authors have no conflicts of interests to declare.

References

Atangana, E., Schneider, U.C., Blecharz, K., Magrini, S., Wagner, J., Nieminen-Kelha, M., Kremenetskaia, I., Heppner, F.L., Engelhardt, B., Vajkoczy, P., 2017. Intravascular

inflammation triggers intracerebral activated microglia and contributes to secondary brain injury after experimental subarachnoid Hemorrhage (eSAH). Transl. Stroke Res. 8 (2), 144–156. https://doi.org/10.1007/s12975-016-0485-3.

Aubrecht, T.G., Faden, A.I., Sabirzhanov, B., Glaser, E.P., Roelofs, B.A., Polster, B.M., Makarevich, O., Stoica, B.A., 2018. Comparing effects of CDK inhibition and E2F1/2 ablation on neuronal cell death pathways in vitro and after traumatic brain injury. Cell Death Dis. 9 (11), 1121. https://doi.org/10.1038/s41419-018-1156-y.

Block, M.L., Hong, J.S., 2005. Microglia and inflammation-mediated neurodegeneration: multiple triggers with a common mechanism. Prog. Neurobiol. 76 (2), 77–98. https://doi.org/10.1016/j.pneurobio.2005.06.004.

Bruun, K., Schermer, E., Sivendra, A., Valaik, E., Wise, R.B., Said, R., Bracht, J.R., 2018. Therapeutic applications of adipose-derived stem cells in cardiovascular disease. Am. J. Stem Cells 7 (4), 94–103.

Calsolaro, V., Edison, P., 2016. Neuroinflammation in Alzheimer's disease: current evidence and future directions. Alzheimers Dement. 12 (6), 719–732. https://doi.org/10.1016/j.jalz.2016.02.010.

Davalos, D., Grutzendler, J., Yang, G., Kim, J.V., Zuo, Y., Jung, S., Littman, D.R., Dustin, M.L., Gan, W.B., 2005. ATP mediates rapid microglial response to local brain injury in vivo. Nat. Neurosci. 8 (6), 752–758. https://doi.org/10.1038/nn1472.

D'Avila, J.C., Lam, T.I., Bingham, D., Shi, J., Won, S.J., Kauppinen, T.M., Massa, S., Liu, J., Swanson, R.A., 2012. Microglial activation induced by brain trauma is suppressed by post-injury treatment with a PARP inhibitor. J. Neuroinflammation 9, 31. https://doi.org/10.1186/1742-2094-9-31.

Doeppner, T.R., Herz, J., Gorgens, A., Schlechter, J., Ludwig, A.K., Radtke, S., de Miroschedji, K., Horn, P.A., Giebel, B., Hermann, D.M., 2015. Extracellular vesicles improve post-stroke Neuroregeneration and prevent Postischemic immunosuppression. Stem Cells Transl. Med. 4 (10), 1131–1143. https://doi.org/10.5966/sctm.2015-0078.

El, A.M., Binder, N., Steffen, R., Schneider, H., Luft, A.R., Weller, M., Imthurn, B., Merki-Feld, G.S., Wegener, S., 2019. Contraceptive drugs mitigate experimental stroke-induced brain injury. Cardiovasc. Res. 115 (3), 637–646. https://doi.org/10.1093/cvr/cvy248.

Fang, B., Song, Y., Liao, L., Zhang, Y., Zhao, R.C., 2007. Favorable response to human adipose tissue-derived mesenchymal stem cells in steroid-refractory acute graft-versus-host disease. Transplant. Proc. 39 (10), 3358–3362. https://doi.org/10.1016/j.transproceed.2007.08.103.

Gadelkarim, M., Abushouk, A.I., Ghanem, E., Hamaad, A.M., Saad, A.M., Abdel-Daim, M.M., 2018. Adipose-derived stem cells: effectiveness and advances in delivery in diabetic wound healing. Biomed. Pharmacother. 107, 625–633. https://doi.org/10.1016/j.biopha.2018.08.013.

Han, Y., Seyfried, D., Meng, Y., Yang, D., Schultz, L., Chopp, M., Seyfried, D., 2018. Multipotent mesenchymal stromal cell-derived exosomes improve functional recovery after experimental intracerebral hemorrhage in the rat. J. Neurosurg. 1–11. https://doi.org/10.3171/2018.2.JNS171475.

Hassani, Z., O'Reilly, J., Pearse, Y., Stroemer, P., Tang, E., Sinden, J., Price, J., Thuret, S., 2012. Human neural progenitor cell engraftment increases neurogenesis and microglial recruitment in the brain of rats with stroke. PLoS ONE 7 (11), e50444. https://doi.org/10.1371/journal.pone.0050444.

Hassanshahi, A., Hassanshahi, M., Khabbazi, S., Hosseini-Khah, Z., Peymanfar, Y., Ghalamkari, S., Su, Y.W., Xian, C.J., 2019. Adipose-derived stem cells for wound healing. J. Cell. Physiol. 234 (6), 7903–7914. https://doi.org/10.1002/jcp.27922.

Helmy, A., De Simoni, M.G., Guilfoyle, M.R., Carpenter, K.L., Hutchinson, P.J., 2011. Cytokines and innate inflammation in the pathogenesis of human traumatic brain injury. Prog. Neurobiol. 95 (3), 352–372. https://doi.org/10.1016/j.pneurobio.2011.09.003.

Hoshino, A., Costa-Silva, B., Shen, T.L., Rodrigues, G., Hashimoto, A., Tesic, M.M., Molina, H., Kohsaka, S., Di Giannatale, A., Ceder, S., Singh, S., Williams, C., Soplop, N., Uryu, K., Pharmer, L., King, T., Bojmar, L., Davies, A.E., Ararso, Y., Zhang, T., Zhang, H., Hernandez, J., Weiss, J.M., Dumont-Cole, V.D., Kramer, K., Wexler, L.H., Narendran, A., Schwartz, G.K., Healey, J.H., Sandstrom, P., Labori, K.J., Kure, E.H., Grandgenett, P.M., Hollingsworth, M.A., de Sousa, M., Kaur, S., Jain, M., Mallya, K., Batra, S.K., Jarnagin, W.R., Brady, M.S., Fodstad, O., Muller, V., Pantel, K., Minn, A.J., Bissell, M.J., Garcia, B.A., Kang, Y., Rajasekhar, V.K., Ghajar, C.M., Matei, I., Peinado, H., Bromberg, J., Lyden, D., 2015. Tumour exosome integrins determine organotropic metastasis. Nature 527 (7578), 329–335. https://doi.org/10.1038/nature15756.

Hsuan, Y.C., Lin, C.H., Chang, C.P., Lin, M.T., 2016. Mesenchymal stem cell-based treatments for stroke, neural trauma, and heat stroke. Brain Behav. 6 (10), e526. https://doi.org/10.1002/brb3.526.

Jaimes, Y., Naaldijk, Y., Wenk, K., Leovsky, C., Emmrich, F., 2017. Mesenchymal stem cell-derived microvesicles modulate lipopolysaccharides-induced inflammatory responses to microglia cells. Stem Cells 35 (3), 812–823. https://doi.org/10.1002/stem.2541.

Koizumi, S., Shigemoto-Mogami, Y., Nasu-Tada, K., Shinozaki, Y., Ohsawa, K., Tsuda, M., Joshi, B.V., Jacobson, K.A., Kohsaka, S., Inoue, K., 2007. UDP acting at P2Y6 receptors is a mediator of microglial phagocytosis. Nature 446 (7139), 1091–1095. https://doi.org/10.1038/nature05704.

Kumar, A., Henry, R.J., Stoica, B.A., Loane, D.J., Abulwerdi, G., Bhat, S.A., Faden, A.I., 2019. Neutral sphingomyelinase inhibition alleviates LPS-induced microglia activation and Neuroinflammation after experimental traumatic brain injury. J. Pharmacol. Exp. Ther. 368 (3), 338–352. https://doi.org/10.1124/jpet.118.253955.

Lauritano, D., Palmieri, A., Candotto, V., Carinci, F., 2018. Regenerative dentistry and stem cells: a multilineage differentiation as a safe and useful alternative way of harvesting and selection adipose derived mesenchymal stem cells. Curr. Drug Targets 19 (16), 1991–1997. https://doi.org/10.2174/1389450119666180816122230.

Lee, M., Ban, J.J., Yang, S., Im, W., Kim, M., 2018. The exosome of adipose-derived stem cells reduces beta-amyloid pathology and apoptosis of neuronal cells derived from the transgenic mouse model of Alzheimer's disease. Brain Res. 1691, 87–93. https://doi.org/10.1016/j.brainres.2018.03.034.

Lee, S.W., de Rivero, V.J., Truettner, J.S., Dietrich, W.D., Keane, R.W., 2019. The role of microglial inflammasome activation in pyroptotic cell death following penetrating traumatic brain injury. J. Neuroinflammation 16 (1), 27. https://doi.org/10.1186/s12974-019-1423-6.

Lener, T., Gimona, M., Aigner, L., Borger, V., Buzas, E., Camussi, G., Chaput, N., Chatterjee, D., Court, F.A., Del, P.H., O'Driscoll, L., Fais, S., Falcon-Perez, J.M., Felderhoff-Mueser, U., Fraile, L., Gho, Y.S., Gorgens, A., Gupta, R.C., Hendrix, A., Hermann, D.M., Hill, A.F., Hochberg, F., Horn, P.A., de Kleijn, D., Kordelas, L., Kramer, B.W., Kramer-Albers, E.M., Laner-Plamberger, S., Laitinen, S., Leonardi, T., Lorenowicz, M.J., Lim, S.K., Lotvall, J., Maguire, C.A., Marcilla, A., Nazarenko, I., Ochiya, T., Patel, T., Pedersen, S., Pocsfalvi, G., Pluchino, S., Quesenberry, P., Reischl, I.G., Rivera, F.J., Sanzenbacher, R., Schallmoser, K., Slaper-Cortenbach, I., Strunk, D., Tonn, T., Vader, P., van Balkom, B.W., Wauben, M., Andaloussi, S.E., Thery, C., Rohde, E., Giebel, B., 2015. Applying extracellular vesicles based therapeutics in clinical trials - an ISEV position paper. J. Extracell. Vesicles 4, 30087. https://doi.org/10.3402/jev.v4.30087.

Li, X., Peng, H., Wu, J., Xu, Y., 2018a. Brain natriuretic peptide-regulated expression of inflammatory cytokines in lipopolysaccharide (LPS)-activated macrophages via NF-kappaB and mitogen activated protein kinase (MAPK) pathways. Med. Sci. Monit. 24, 3119–3126. https://doi.org/10.12659/MSM.905580.

Li, X., Wang, T., Zhang, D., Li, H., Shen, H., Ding, X., Chen, G., 2018b. Andrographolide ameliorates intracerebral hemorrhage induced secondary brain injury by inhibiting neuroinflammation induction. Neuropharmacology 141, 305–315. https://doi.org/10.1016/j.neuropharm.2018.09.015.

Li, X., Xie, X., Lian, W., Shi, R., Han, S., Zhang, H., Lu, L., Li, M., 2018c. Exosomes from adipose-derived stem cells overexpressing Nrf2 accelerate cutaneous wound healing by promoting vascularization in a diabetic foot ulcer rat model. Exp. Mol. Med. 50 (4), 29. https://doi.org/10.1038/s12276-018-0058-5.

Liang, X., Ding, Y., Zhang, Y., Tse, H.F., Lian, Q., 2014. Paracrine mechanisms of mesenchymal stem cell-based therapy: current status and perspectives. Cell Transplant. 23 (9), 1045–1059. https://doi.org/10.3727/096368913X667709.

Liu, X.L., Zhang, W., Tang, S.J., 2014. Intracranial transplantation of human adipose-derived stem cells promotes the expression of neurotrophic factors and nerve repair in rats of cerebral ischemia-reperfusion injury. Int. J. Clin. Exp. Pathol. 7 (1), 174–183.

Liu, H., Hua, Y., Keep, R.F., Xi, G., 2019. Brain Ceruloplasmin expression after experimental intracerebral Hemorrhage and protection against iron-induced brain injury. Transl. Stroke Res. 10 (1), 112–119. https://doi.org/10.1007/s12975-018-0669-0.

Lv, B., Hua, T., Li, F., Han, J., Fang, J., Xu, L., Sun, C., Zhang, Z., Feng, Z., Jiang, X., 2017a. Hypoxia-inducible factor 1 alpha protects mesenchymal stem cells against oxygen-glucose deprivation-induced injury via autophagy induction and PI3K/AKT/mTOR signaling pathway. Am. J. Transl. Res. 9 (5), 2492–2499.

Lv, B., Hua, T., Li, F., Han, J., Fang, J., Xu, L., Sun, C., Zhang, Z., Feng, Z., Jiang, X., 2017b. Hypoxia-inducible factor 1 alpha protects mesenchymal stem cells against oxygen-glucose deprivation-induced injury via autophagy induction and PI3K/AKT/mTOR signaling pathway. Am. J. Transl. Res. 9 (5), 2492–2499. https://doi.org/10.3389/fnmol.2017.00080.

Ma, T., Gong, K., Ao, Q., Yan, Y., Song, B., Huang, H., Zhang, X., Gong, Y., 2013. Intracerebral transplantation of adipose-derived mesenchymal stem cells alternatively activates microglia and ameliorates neuropathological deficits in Alzheimer's disease mice. Cell Transplant. 22 (Suppl. 1), S113–S126. https://doi.org/10.3727/096368913X672181.

Ni, H., Yang, S., Siaw-Debrah, F., Hu, J., Wu, K., He, Z., Yang, J., Pan, S., Lin, X., Ye, H., Xu, Z., Wang, F., Jin, K., Zhuge, Q., Huang, L., 2019. Exosomes derived from bone mesenchymal stem cells ameliorate early inflammatory responses following traumatic brain injury. Front. Neurosci. 13, 14. https://doi.org/10.3389/fnins.2019.00014.

Nimmerjahn, A., Kirchhoff, F., Helmchen, F., 2005. Resting microglial cells are highly dynamic surveillants of brain parenchyma in vivo. Science 308 (5726), 1314–1318. https://doi.org/10.1126/science.1110647.

Pan, J., Alimujiang, M., Chen, Q., Shi, H., Luo, X., 2019. Exosomes derived from miR-146a-modified adipose-derived stem cells attenuate acute myocardial infarction-induced myocardial damage via downregulation of early growth response factor 1. J. Cell. Biochem. 120 (3), 4433–4443. https://doi.org/10.1002/jcb.27731.

Pedersen, K.W., Kierulf, B., Neurauter, A., 2017. Specific and generic isolation of extracellular vesicles with magnetic beads. Methods Mol. Biol. 1660, 65–87. https://doi.org/10.1007/978-1-4939-7253-1_7.

Peinado, H., Aleckovic, M., Lavotshkin, S., Matei, I., Costa-Silva, B., Moreno-Bueno, G., Hergueta-Redondo, M., Williams, C., Garcia-Santos, G., Ghajar, C., Nitadori-Hoshino, A., Hoffman, C., Badal, K., Garcia, B.A., Callahan, M.K., Yuan, J., Martins, V.R., Skog, J., Kaplan, R.N., Brady, M.S., Wolchok, J.D., Chapman, P.B., Kang, Y., Bromberg, J., Lyden, D., 2012. Melanoma exosomes educate bone marrow progenitor cells toward a pro-metastatic phenotype through MET. Nat. Med. 18 (6), 883–891. https://doi.org/10.1038/nm.2753.

Ratajczak, J., Wysoczynski, M., Hayek, F., Janowska-Wieczorek, A., Ratajczak, M.Z., 2006. Membrane-derived microvesicles: important and underappreciated mediators of cell-to-cell communication. Leukemia 20 (9), 1487–1495. https://doi.org/10.1038/sj.leu.2404296.

Sierra, A., Encinas, J.M., Deudero, J.J., Chancey, J.H., Enikolopov, G., Overstreet-Wadiche, L.S., Tsirka, S.E., Maletic-Savatic, M., 2010. Microglia shape adult hippocampal neurogenesis through apoptosis-coupled phagocytosis. Cell Stem Cell 7 (4), 483–495. https://doi.org/10.1016/j.stem.2010.08.014.

Tajiri, N., Acosta, S.A., Shahaduzzaman, M., Ishikawa, H., Shinozuka, K., Pabon, M.,

Hernandez-Ontiveros, D., Kim, D.W., Metcalf, C., Staples, M., Dailey, T., Vasconcellos, J., Franyuti, G., Gould, L., Patel, N., Cooper, D., Kaneko, Y., Borlongan, C.V., Bickford, P.C., 2014. Intravenous transplants of human adipose-derived stem cell protect the brain from traumatic brain injury-induced neurodegeneration and motor and cognitive impairments: cell graft biodistribution and soluble factors in young and aged rats. J. Neurosci. 34 (1), 313–326. https://doi.org/10.1523/JNEUROSCI.2425-13.2014.

Tominaga, N., Kosaka, N., Ono, M., Katsuda, T., Yoshioka, Y., Tamura, K., Lotvall, J., Nakagama, H., Ochiya, T., 2015. Brain metastatic cancer cells release microRNA-181c-containing extracellular vesicles capable of destructing blood-brain barrier. Nat. Commun. 6, 6716. https://doi.org/10.1038/ncomms7716.

Waisman, A., Ginhoux, F., Greter, M., Bruttger, J., 2015. Homeostasis of microglia in the adult brain: review of novel microglia depletion systems. Trends Immunol. 36 (10), 625–636. https://doi.org/10.1016/j.it.2015.08.005.

Wang, B., Han, S., 2018. Modified exosomes reduce apoptosis and ameliorate neural deficits induced by traumatic brain injury. ASAIO J. https://doi.org/10.1097/MAT.0000000000000810.

Wang, H., Bi, C., Wang, Y., Sun, J., Meng, X., Li, J., 2018. Selenium ameliorates Staphylococcus aureus-induced inflammation in bovine mammary epithelial cells by inhibiting activation of TLR2, NF-kappaB and MAPK signaling pathways. BMC Vet. Res. 14 (1), 197. https://doi.org/10.1186/s12917-018-1508-y.

Wu, R., Li, X., Xu, P., Huang, L., Cheng, J., Huang, X., Jiang, J., Wu, L.J., Tang, Y., 2017. TREM2 protects against cerebral ischemia/reperfusion injury. Mol. Brain 10 (1), 20. https://doi.org/10.1186/s13041-017-0296-9.

Wu, Z., Wang, L., Li, J., Wang, L., Wu, Z., Sun, X., 2018. Extracellular vesicle-mediated communication within host-parasite interactions. Front. Immunol. 9, 3066. https://doi.org/10.3389/fimmu.2018.03066.

Xu, H., Qin, W., Hu, X., Mu, S., Zhu, J., Lu, W., Luo, Y., 2018. Lentivirus-mediated overexpression of OTULIN ameliorates microglia activation and neuroinflammation by depressing the activation of the NF-kappaB signaling pathway in cerebral ischemia/reperfusion rats. J. Neuroinflammation 15 (1), 83. https://doi.org/10.1186/s12974-018-1117-5.

Yang, J., Zhang, X., Chen, X., Wang, L., Yang, G., 2017. Exosome mediated delivery of miR-124 promotes neurogenesis after ischemia. Mol. Ther. Nucleic Acids 7, 278–287. https://doi.org/10.1016/j.omtn.2017.04.010.

Yang, Y., Cai, Y., Zhang, Y., Liu, J., Xu, Z., 2018. Exosomes secreted by adipose-derived stem cells contribute to angiogenesis of brain microvascular endothelial cells following oxygen-glucose deprivation in vitro through MicroRNA-181b/TRPM7 Axis. J. Mol. Neurosci. 65 (1), 74–83. https://doi.org/10.1007/s12031-018-1071-9.

Yang, Y., Ye, Y., Kong, C., Su, X., Zhang, X., Bai, W., He, X., 2019. MiR-124 enriched exosomes promoted the M2 polarization of microglia and enhanced Hippocampus neurogenesis after traumatic brain injury by inhibiting TLR4 pathway. Neurochem. Res. https://doi.org/10.1007/s11064-018-02714-z.

Zhang, J., Zhou, S., Zhou, Y., Feng, F., Wang, Q., Zhu, X., Ai, H., Huang, X., Zhang, X., 2014. Hepatocyte growth factor gene-modified adipose-derived mesenchymal stem cells ameliorate radiation induced liver damage in a rat model. PLoS ONE 9 (12), e114670. https://doi.org/10.1371/journal.pone.0114670.

Zhang, Z., Yang, C., Shen, M., Yang, M., Jin, Z., Ding, L., Jiang, W., Yang, J., Chen, H., Cao, F., Hu, T., 2017. Autophagy mediates the beneficial effect of hypoxic preconditioning on bone marrow mesenchymal stem cells for the therapy of myocardial infarction. Stem Cell Res. Ther. 8 (1), 89. https://doi.org/10.1186/s13287-017-0543-0.

Zhao, L., Johnson, T., Liu, D., 2017. Therapeutic angiogenesis of adipose-derived stem cells for ischemic diseases. Stem Cell Res. Ther. 8 (1), 125. https://doi.org/10.1186/s13287-017-0578-2.